Icarus 199 (2009) 378–386

Contents lists available at ScienceDirect

Icarus

www.elsevier.com/locate/icarus

Three tenuous rings/arcs for three tiny moons

M.M. Hedman [a,*], C.D. Murray [b], N.J. Cooper [b], M.S. Tiscareno [a], K. Beurle [b], M.W. Evans [b], J.A. Burns [a,c]

[a] Department of Astronomy, Cornell University, Ithaca, NY 14853, USA
[b] Queen Mary University of London, Astronomy Unit, Mile End Road, London E1 4NS, United Kingdom
[c] Department of Theoretical and Applied Mechanics, Cornell University, Ithaca, NY 14853, USA

ARTICLE INFO

Article history:
Received 7 August 2008
Revised 6 November 2008
Accepted 10 November 2008
Available online 25 November 2008

Keywords:
Saturn, rings
Saturn, satellites
Resonances, rings

ABSTRACT

Using Cassini images, we examine the faint material along the orbits of Methone, Anthe and Pallene, three small moons that reside between the orbits of Mimas and Enceladus. A continuous ring of material covers the orbit of Pallene; it is visible at extremely high phase angles and appears to be localized vertically to within ±25 km of Pallene's inclined orbit. By contrast, the material associated with Anthe and Methone appears to lie in longitudinally confined arcs. The Methone arc extends over ∼10° in longitude around the satellite's position, while the Anthe arc reaches ∼20° in length. The extents of these arcs are consistent with their confinement by nearby corotation eccentricity resonances with Mimas. Anthe has even been observed to shift in longitude relative to its arc in the expected manner given the predicted librations of the moon.

1. Introduction

Since Cassini arrived at Saturn in the summer of 2004, it has made many discoveries—some are tangible, such as five new moons (Daphnis, Anthe, Methone, Pallene and Polydeuces) and several new rings, while others are conceptual, such as an improved understanding of the interaction between moons and nearby rings (e.g., Porco et al., 2007; Charnoz et al., 2007; Murray et al., 2008). The data described here can be counted among both of these sorts of discoveries: they are the first images of three previously unseen rings, but they also document novel relationships between small moons and low-optical-depth material.

The rings discussed here are localized near the orbits of Methone, Anthe and Pallene, three small moons of Saturn whose orbits lie between those of Mimas and Enceladus. The ability of such small moons to generate rings has been a subject of interest for some time (cf. Burns et al., 1999, 2004), and examples of faint rings interacting with similarly small moons have been found around all the giant planets: Jupiter (Burns et al., 1999, 2004; Showalter et al., 2007), Saturn (Porco et al., 2007; Murray et al., 2008), Uranus (Showalter and Lissauer, 2006) and Neptune (de Pater et al., 2005). However, evidence that these particular saturnian moons do in fact produce faint rings has only recently become available. Images of a ring associated with Pallene, charged-particle absorptions ascribed to material near Methone, and images of arcs associated with both Anthe and Methone were announced in the last two years (Porco et al., 2006a; Roussos et al., 2006; Porco et al., 2008).

After reviewing prior in situ evidence for material associated with at least one of these moons, this paper will describe the structure of the rings associated with Pallene, Methone and Anthe as they have been observed by Cassini's cameras. After this, we discuss of how the variety of structures seen in these rings can be understood in terms of the detailed dynamical environments of the relevant moons. Note that this paper does not consider here the faint ring which lies near the orbits of Janus and Epimetheus (Porco et al., 2006a). These moons' much larger masses and their unique co-orbital resonant configuration make the dynamics of their ring a special case that is beyond the scope of this paper.

2. Previous detections of material associated with Methone

Before discussing the images of these rings, we must first mention the in situ measurements of charged particle absorptions that provided the earliest evidence for dispersed material associated with these moons. Historically, charged particle absorption signatures have often provided the first hints of low-optical depth rings. For example, Jupiter's ring was first suggested when Pioneer 10 detected low energetic-particle fluxes inwards of Amalthea's orbit (Acuna and Ness, 1976) and Saturn's G ring was detected through its modest reduction in several species of charged particles as measured by Pioneer 11 (cf. van Allen, 1983). In both these cases subsequent imaging confirmed the existence of rings in these locations. More recently, a combination of in situ and remote-sensing data of the arc in the G ring yielded a consistent model for the origin of this ring (Hedman et al., 2007). However, there are

* Corresponding author.
E-mail address: mmhedman@astro.cornell.edu (M.M. Hedman).

0019-1035/$ – see front matter
doi:10.1016/j.icarus.2008.11.001

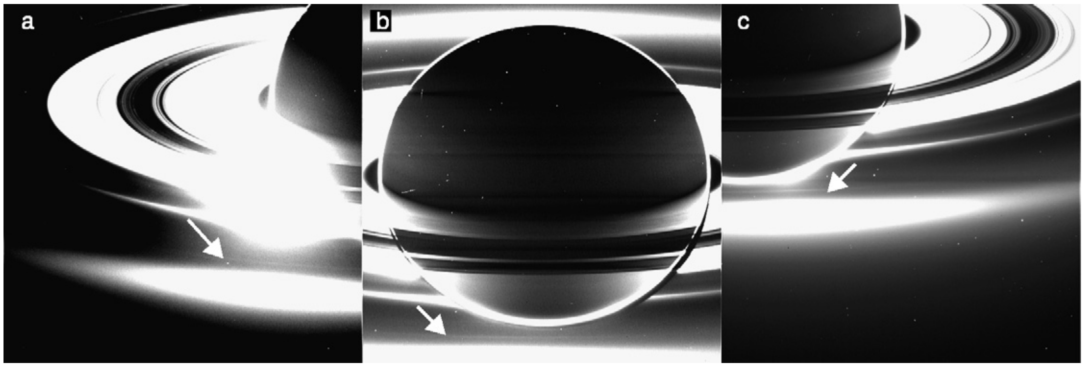

Fig. 1. Representative images of the Pallene ring obtained during the Day 258 of 2006 eclipse observations: (a) W1537005302 from the HIPHASE001 sequence; (b) W1537028814 from the HIPHWAC001 sequence; (c) W1537050260 from the HIPHASE002 sequence. All images were taken with the Wide-Angle Camera (WAC) using the VIO filter. The brightness scales are individually stretched for presentation. These three images were obtained at 9:23, 15:55 and 21:52 UTC, respectively. In all three images the Pallene ringlet (marked with an arrow) is most visible just off Saturn's southern limb, where the phase angle is highest.

also instances (Chenette and Stone, 1983; Cuzzi and Burns, 1988; Jones et al., 2008; Kerr, 2008) where the connection between the in situ measurements and visible rings is more uncertain and controversial.

The in situ measurements relevant to this work consist of two absorption signatures of ∼MeV-electrons that have been identified in three channels of MIMI/LEMMS data obtained very close to Methone's L-shell (i.e. where magnetic field lines threading the spacecraft pass close to Methone's orbit). These absorptions occurred when the satellite was "upstream" and longitudinally nearby the magnetic field lines connected to the spacecraft (Roussos et al., 2008). The inbound and outbound microsignatures are each tens of percent deep and have radial extents of 2400 km and 1500 km, respectively. The inbound signature was separated by 17° from Methone and lay nearly 5000 km exterior to Methone's L-shell, whereas the outbound depletion was separated by about 5° from Methone and occurred exactly on the satellite's L-shell. Because Methone is so small and inert, by itself the moon is not likely to generate a >1000-km wide signature. Roussos et al. (2008) instead investigate the possibility of a dust arc, treating it in the manner of Cuzzi and Burns (1988). They conclude that a 15°-long arc comprised of particles larger than a mm and with an optical depth lower than the E or G rings ($\sim 10^{-6}$) would provide a sufficient obstacle to account for the observed absorption. As described below, imaging data now confirm such material does in fact exist around Methone.

The radial shift of the inbound detection relative to Methone's L-shell is not easily explained (Roussos et al., 2008). This shift results in the absorption occurring closer to Anthe's L-shell, so an arc of material in that moon's orbit could possibly explain that absorption. However, the images discussed below show that the material associated with Methone and Anthe are organized into longitudinally-confined arcs 10–20 degrees across. Anthe was over 120° from Cassini when these absorptions were observed, and while microsignature identification can be a complex problem, we think it is more likely that both signatures are due to Methone. We may also note in passing that there are other cases, notably including the G-ring arc detection (Hedman et al., 2007), where similarly puzzling radial displacements are seen.

3. Imaging observations

The images discussed here were obtained by the Imaging Science Subsystem (ISS) onboard the Cassini spacecraft. This consists of a Narrow-Angle Camera (NAC) and Wide-Angle Camera (WAC), each of which is equipped with multiple color filters (Porco et al., 2004). All images are initially processed using the CISSCAL calibration routines (Porco et al., 2004) that remove backgrounds, flatfield the images, and convert the raw data numbers into I/F, a standardized measure of reflectance. I is the intensity of the scattered radiation while πF is the solar flux at Saturn, so I/F is a unitless quantity that equals unity for a perfect Lambert surface viewed at normal incidence. Note that these automated routines do not eliminate all instrumental artifacts in the images, and so additional processing is often needed to extract information about faint features like those discussed here.

In order to facilitate comparisons between observations taken from different elevation angles, we often convert the observed I/F values to "normal I/F" $= \mu I/F$, where μ is the cosine of the emission angle. The normal I/F should be independent of emission angle so long as $\tau/\mu \ll 1$ (where τ is the ring's normal optical depth) and the ring opening angle is sufficiently high that the vertical width of the ring can be neglected. While the former is certainly true for these faint rings, the latter condition is likely violated in some of the nearly edge-on images.

The images containing the Pallene ring happen to have been taken at extremely high phase angles (>175°) or extremely low ring opening angles (<0.5°), while the images containing the Methone and Anthe rings are at relatively low phase angles (<50°). We therefore will consider the Pallene ring observations separately from those of the Anthe and Methone rings below.

3.1. Pallene ring

The Pallene ring is seen most clearly in images obtained by Cassini on Day 258 of 2006, when the spacecraft flew through Saturn's shadow and was therefore permitted to observe the rings at extremely high phase angles (>175°). While the cameras obtained images through a number of different filters, we will only consider here the images taken through the short-wavelength VIO filter (effective central wavelength 420 nm). These images are the most useful for studying the morphology of faint structures like the Pallene ring because various artifacts due to scattered light in the optics are least prominent at these wavelengths. Furthermore, these images are the least likely to exhibit "bleeding" due to hyper-saturation of the image on the bright limb of the planet. The images taken through the VIO-filter therefore provide us with the "cleanest" pictures of the Pallene ring. (Images from other filters will be used in a later paper describing the spectrophotometric properties of such faint rings.)

Fig. 1 shows representative VIO-filter images taken during this time period. All these images show a bright ring with a full-width at half-maximum of approximately 2500 km located roughly 212,000 km from Saturn's center, near the orbit of Pallene. This ringlet is only clearly visible above the background in these images at phase angles above 178°, so the full longitudinal extent of